

# Organic and Ceramic SoP Solutions and Modules for mmW Applications

Manos M. Tentzeris

ECE/GEDC, Georgia Tech, Atlanta, GA 30332-250

Email: etentze@ece.gatech.edu

**ABSTRACT** — In this paper, fully integrated filter and antenna functions are demonstrated as a system-on-package (SOP) compact front-end solutions for the low-temperature cofired ceramic (LTCC) and for Liquid-Crystal Polymer (LCP) based millimeter-wave modules. The compact and easy-to-design integrated passive functions of filter and antenna have been hereby experimentally validated. The above proposed designs can be easily combined, leading to the complete passive integration with high level of selectivity over the band of interest.

**Index Terms** — Ceramics, organics, flexible electronics, RF modules, 3D integration, millimeter-wave.

## I. INTRODUCTION

The dramatic increase of interest in license-free spectrum around 60 GHz is led by the high-data rate applications such as high-speed internet access, video streaming, content downloads, and wireless data bus for cable replacement. Such emerging applications with data rate greater than 2 Gb/s require real estate efficiency, low-cost manufacturing, and excellent performance achieved by a high level of integration of embedded functions using low-cost and high-performance materials such as the multilayer low-temperature cofired ceramic (LTCC) [1-2]. The optimal integration of RF passives into 60 GHz (V-band) front-end module is significantly challenging since the electrical performance can be degraded by severe parasitic and interconnection losses. The microwave structures for integrating filter and antenna function which is commonly called a filtering antenna have been implemented using stacked cavities coupled by a metallic iris at K-band, an electromagnetic horn and a leaky waveguide at X-band. Despite of their large size, these topologies show that the integrated filter and antenna functions have a great potential to be integrated into higher frequencies modules.

In this paper, we present compact and high-performance passive building blocks and their integration, enabling a complete passive integration solution for 3D compact, low-cost wireless V-band front-end modules. The section II of this paper discusses the development of a 4-pole cross-coupled quasi-elliptic filter, targeting high selectivity and compactness. Section III concentrates on the design of a series fed  $1 \times 4$  linear array antenna of four micro-strip patches covering 59-64 GHz. This high-gain

and directive antenna is suited for point-to-point applications in short-range indoor wireless personal area network (WPAN) and can be easily integrated into a V-band module. The complete integration of the above developed filter and antenna was successfully implemented with a planar transition as described in section III. The integrated front-end demonstrates the excellent band selectivity through a 10-dB bandwidth of approximately 4.8 GHz (59.2 – 64 GHz) and return loss  $>10.47$  dB over the passband.

Liquid crystal polymer has gained considerable press for several reasons. It has “best of the polymers” packaging characteristics, excellent electrical properties, and many other notable qualities [3]. The material was made commercially available in double copper clad thin films for the first time in 2003 and has made large strides in its multilayer fabrication capabilities. A simplified end goal of such progress is to create multilayer LCP boards that have a homogeneous dielectric makeup throughout (no epoxies or other bonding materials). This goal would certainly be more enticing if the functionality of embedded monolithic integrated circuits (MMICs) could be shown to be compatible with a multilayer lamination process. Unfortunately, with LTCC, the lamination temperature ( $>800^\circ\text{C}$ ) is well above the threshold which destroys integrated circuits. If both active and passive components could be shown compatible with a multilayer LCP lamination process, a new class of near-hermetic RF systems in a compact, relatively low-cost topology could be realized. The process of embedding an active device in LCP, forming a useful package from several LCP layers, and testing the survivability of MMICs during the LCP lamination temperature profile are the topics of this paper.

## II. LTCC 4-POLE QUASI-ELLIPTIC FILTER

As the demand for highly selective, compact and low loss band pass filters increases in multi-gigabit-per-second wireless communication systems, the coupled open-loop resonator filter becomes a candidate of choice for the integration of V-band front-end modules. Numerous researchers have demonstrated narrow bandwidth filters employing open-loop resonators for current mobile communication services at L and S bands. In this section,

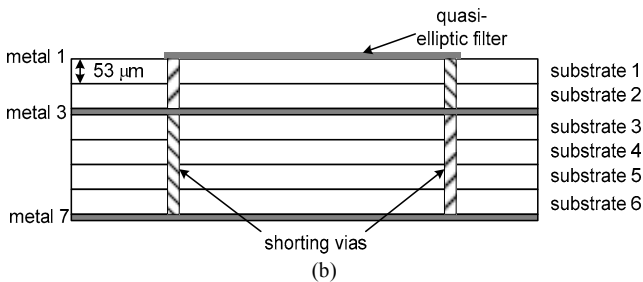
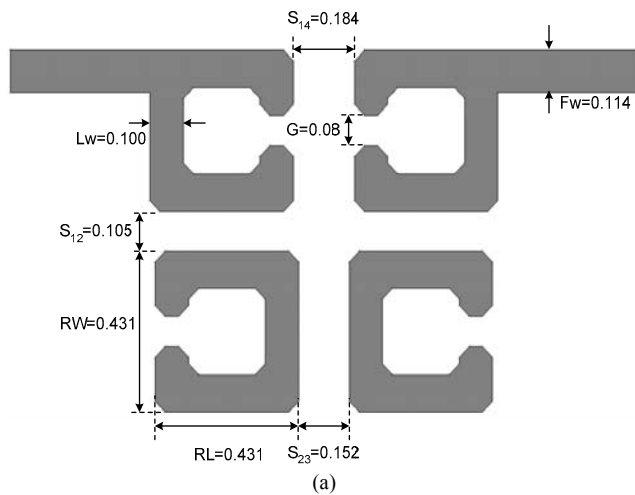


Figure 1. (a) Top view and (b) cross-section view of 4-pole quasi-elliptic band pass filter consisting of open-loop resonators fabricated on LTCC. All dimensions indicated in (a) are in mm.

the design of a 4-pole quasi-elliptic filter is presented as a filter solution for LTCC 60 GHz front-end module. This filter is chosen because it provides only one pair of transmission zeros at finite frequencies to satisfy the desired specifications (listed below), exhibiting much improved skirt selectivity and making it a feasible intermediate between the Chebyshev and elliptical-function filters]. At millimeter-wave frequencies, the design of the coupled open-loop resonator filter is very challenging because of the design rules limitations of the process. Nevertheless, the very mature multilayer fabrication capabilities of LTCC ( $\epsilon_r=7.1$ ,  $\tan\delta=0.0019$ , metal layer thickness:  $9\ \mu\text{m}$ , number of layers: 6, dielectric layer thickness:  $53\ \mu\text{m}$ , minimum metal line width and spacing: up to  $75\ \mu\text{m}$ ) appear to be a competitive solution to meet millimeter-wave design requirements in terms of physical dimension of the open-loop resonators ( $\approx 0.2\lambda_g \times 0.2\lambda_g$ ) and spacing ( $\geq 80\ \mu\text{m}$ ) between adjacent resonators that determine the coupling coefficient of the filter function.

All designs have been simulated using the MOM-based, 2.5 full-wave solver IE3D. Fig. 1 (a), (b) shows the top view and cross-section view of the quasi-elliptic band pass filter, respectively. The filter was designed according to the filter synthesis to meet the following specifications: (1) center frequency: 62 GHz (2) fractional

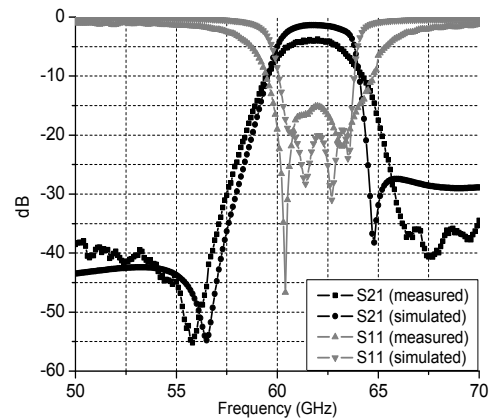


Figure 2. The comparison between measured and simulated S-parameters (S21 & S11) of the 4-pole quasi-elliptic band pass filter composed of open-loop resonators.

bandwidth: 5.61% ( $\sim 3.5\text{GHz}$ ) (3) insertion loss:  $< 3\text{dB}$  (4) 35 dB rejection bandwidth: 7.4 GHz. The effective length (RL in Fig 1 (a)) and width (RW in Fig 1 (a)) of the open resonator has been chosen to be equal to  $0.2\lambda_g$ . The design parameters such as the coupling coefficients ( $C_{12}$ ,  $C_{23}$ ,  $C_{34}$ ,  $C_{14}$ ) and the external quality factor ( $Q_{\text{ext}}$ ) can be theoretically calculated based on the element values of a 4-pole low-pass prototype. The calculated design parameters are:

$$C_{12}=C_{34}=0.048, C_{14}=-0.012$$

$$C_{23}=0.044, Q_{\text{ext}}=17.001.$$

To determine the physical spacing between resonators, full-wave simulations (IE3D) were used to extract the coupling coefficients and external quality factors. The quasi elliptic filter was fabricated on the first metallization layer (metal 1 in Fig 1. (b)), which is placed two substrate layers ( $\sim 106\ \mu\text{m}$ ) above the first ground plane on metal 3. This ground plane is connected to the second ground plane located on the back side of the substrate through shorting vias (pitch:  $390\ \mu\text{m}$ , diameter:  $130\ \mu\text{m}$ ) as shown in Fig. 1 (b). The fabricated filter occupies  $3.075 \times 1.455 \times 0.106\ \text{mm}^3$  ( $\sim 1.40\lambda_g \times 0.66\lambda_g \times 0.048\lambda_g$ ) including feeding structures and CPW measurement pads.

Fig. 2 shows the comparison between the simulated and measured S parameters of the band pass filter. The filter exhibits an insertion loss  $< 3.48\ \text{dB}$  which is higher than the simulated values of  $< 1.37\ \text{dB}$  and a return loss  $> 15\ \text{dB}$  compared to a simulated value of  $< 21.9\ \text{dB}$  over the passband. The loss discrepancy can be attributed to conductor loss caused by skin and edge effect of metal traces since the simulations assume a perfect definition of metal strips. The measurement shows a slightly decreased 3-dB fractional bandwidth of 5.46 % ( $\sim 3.4\ \text{GHz}$ ) at a center frequency of 62.3 GHz. The simulated results give

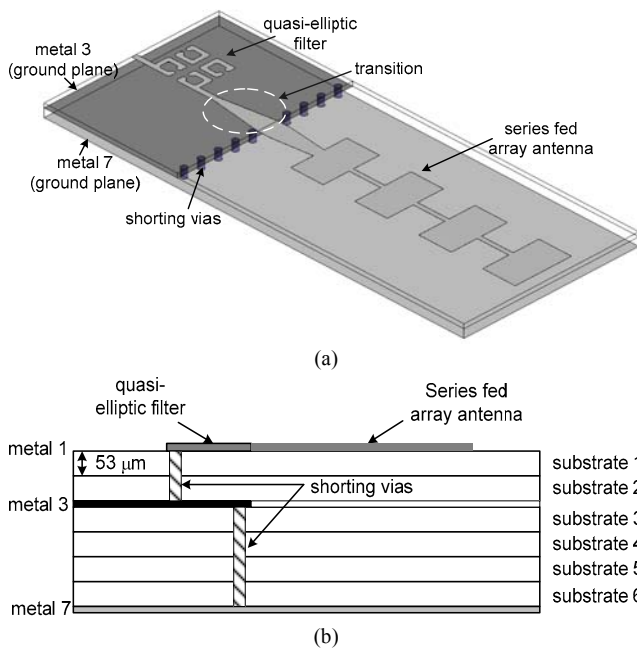


Figure 3. (a) The 3D overview and (b) cross-section view of the integrated filter and antenna functions. All dimensions indicated are in mm.

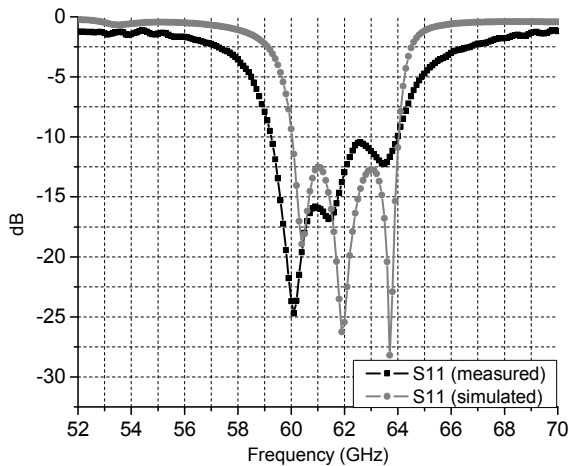


Figure 4. The comparison between measured and simulated return loss (S11) of the integrated filter and antenna functions

a 3 dB bandwidth of 5.61 % (~3.5 GHz) at a center frequency 62.35 GHz. The transmission zeros are observed within < 5 GHz away from the cut-off frequency of the passband. The discrepancy of the zero positions between the measurement and the simulation can be attributed to the fabrication tolerance. However, the overall response of the measurement correlates very well with the simulation.

### III. LTCC MODULE-LEVEL INTEGRATION

In 60 GHz front-end module development, the compact integration of the antenna and filter is a crucial issue in terms of real estate efficiency and performance improvement such as high level of band selectivity,

spurious suppression and low filtering loss.

Using the developed quasi-elliptic filter and the series-fed 4x1 array antenna, it is now possible to realize a V-band compact integrated front-end. The 3D overview and cross-section view of the topology chosen for the integration are shown in Fig. 3 (a) and (b) respectively. The 4-pole quasi-elliptic filter and the 1×4 series fed array antenna are located on the top metallization layer (metal1 in Fig. 3 (b)) and are connected together with a tapered microstrip transition as shown in Fig 3 (a). The ground planes of the filter and the antenna are located on metal 3, on metal 7, respectively. The ground plane of the filter is terminated at the edge of the antenna feedline, and the two ground planes on metal 3 and 7 are connected together with a via array as presented in Fig. 5. The design of the tapered microstrip transition aims to annihilate the parasitic modes from the 50 Ω microstrip lines discontinuities between the two devices and to maintain a good impedance matching. The fabricated integrated front-end occupies an area of  $9.616 \times 1.542 \times 0.318 \text{ mm}^3$  including CPW measurement pads.

Fig. 4 shows the simulated and measured return losses of the integrated structure. It is observed that the 10-dB return loss bandwidth is approximately 4.8 GHz (59.2 – 64 GHz) that is slightly wider than the simulation of 4 GHz (60-64 GHz). The slightly increased bandwidth may be attributed to the parasitic radiation from the feedlines and from the transition, as well as from the edges effects of the discontinuous ground planes.

### IV. LCP EMBEDDING OF ACTIVES

To show the validity of LCP as a lower-cost flexible (but lower hermeticity than LTCC) alternative for mm-wave applications, we show the packaging of a component with a reasonably high frequency range. The die should have compatible dimensions with the planned fabrication processes and the number of input/output connections for wire bonds was desired to be as low as possible for ease of assembly. These requirements pointed roughly in the direction of testing either a GaAs amplifier or oscillator. An oscillator is generally more stable to impedance mismatches from external wire bond and package parasitics. However, a packaged circuit that is more sensitive to external matching is potentially more informative as an indicator of the package utility. That reasoning shifted the decision to a 13-25 GHz low noise amplifier die (model HMC342 from Hittite). This chip was selected since it was one of their smallest chips (2.02 mm x 1.06 mm) and it has the simplest connection (input, output, and one DC bias pad). Also, the 4 mil die thickness was perfect for embedding into a cavity in a commercially available 4 mil LCP sheet. And since GaAs is used well into the mm-wave spectrum, this is a die type that can be used for a wide variety components and

frequency ranges. An off chip bypass capacitor was one further component required by amplifier. The same requirements as before led to a 17 mil x 14 mil x 5 mil thick (0.43 mm x 0.36 mm x 0.13 mm) 130 pF parallel plate bypass capacitor from Presidio Components Inc.

Since LCP comes commercially in 1-, 2-, and 4-mil thicknesses, the layers will require stacking to achieve the necessary thickness and cavity topology to encase an active device. A cavity must be formed above the chip so that the wire bonds have sufficient space to connect from the chip pads to the feeding transmission lines. This vertical clearance is also important since in our final topology the bypass capacitor is 1 mil thicker than the die. In addition, both components will be elevated slightly by the electrically conductive cured silver paste that connects the components to the RF ground plane. Based on a lenient fabrication tolerance budget, on HFSS simulations, and on available LCP thicknesses, the final package test topology is shown in Fig. 5.

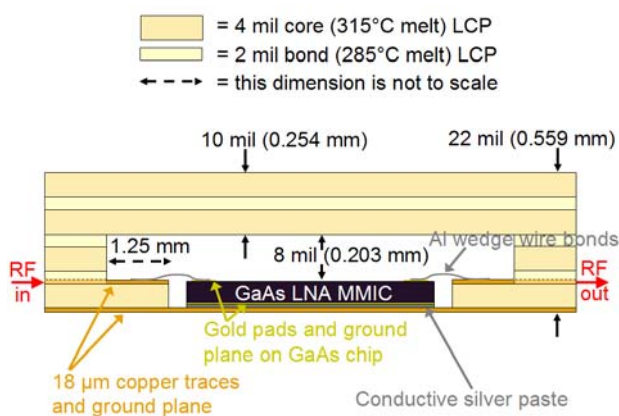


Figure 5. Side view of LCP package stackup.

The LNA was first measured without the packaging layers, then with the packaging layers held in place mechanically, and finally after being subjected to an LCP thermocompression bonding temperature profile. The temperature process was administered on a hotplate and monitored with a Fluke 54II digital thermocouple with an Omega brand probe. The LCP bonding temperature profile rules available from the Rogers website were followed with the exception of the ramp rates for heating and cooling, which were done faster in the interest of time. The LCP package stackup with the GaAs amplifier inside were held together between the aluminum alignment plates and heated and held between 280°C and 285°C for a soak time of 30 minutes. The chip was then re-measured and compared to the original measurements and also to the manufacturer's measurement specification as seen in Fig. 6. The result shows that the gain produced by the chip after the temperature exposure is nearly identical to

that before it up to 18 GHz and it only varies by ~ 0.5 dB through the rest of the band. In addition, all of the measurements are close to the manufacturer's specification with and without the package layers in place. This result of a well working MMIC after the LCP lamination temperature process is good news since the soak temperature isn't far from the manufacturer's 320°C temperature warning, at which a chip will supposedly be destroyed if held for >20 seconds.

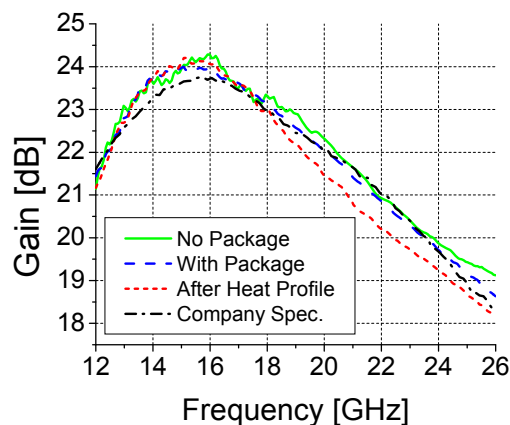


Figure 6. Gain measurement of the Hittite HMC342 13–25 GHz LNA. The chip measures nearly identically before and after the package is introduced.

## VII. CONCLUSION

In this paper, we have presented examples of organic and ceramic multilayer structures for millimeter-wave applications. More complex geometries will be discussed at the conference.

## REFERENCES

- [1] J.-H.Lee, N.Kidera, G.DeJean, S.Pinel, J.Laskar, and M.M.Tentzeris, "A V-Band Front-End with 3D Integrated Cavity Filters/Duplexers and Antenna in LTCC Technologies", IEEE Transactions on Microwave Theory and Techniques, Vol.54, No.7, pp.2925-2936, July 2006.
- [2] J.-H.Lee, S.Pinel, J.Laskar, and M.M.Tentzeris, "Design and Development of Advanced Cavity-Based Dual-Mode Filters Using Low-Temperature Co-Fired Ceramic Technology for V-band Gigabit Wireless Systems", IEEE Transactions on Microwave Theory and Techniques, Vol.55, No.9, pp.1869-1879, September 2007.
- [3] M.M.Tentzeris et al. "3D Integrated RF and Millimeter-Wave Functions and Modules Using Liquid Crystal Polymer (LCP) System-on-Package Technology", IEEE Transactions on Advanced Packaging, Vol.27 No.2, pp.332-340, May 2004.
- [4] A.Rida, A.Margomenos and M.M.Tentzeris, "Novel Wideband 3D Transitions on LCP for Millimeter-Wave Applications up to 100 GHz", Proc. IEEE International Microwave Symp. (IMS2009), Boston, MA, June 2009